International Journal of Advanced Research in Science, Engineering and Technology

ISSN: 2350-0328

Vol. 12, Special Issue, December 2025

National Conference on Earth, Elements and Energy: Interdisciplinary Perspectives (NC3EIP–2025)

IJARSET IMPACT FACTOR 7.150

Preparation and Characterization of SnO_2, WO_3 and SnO_2- WO_3 Hybrid Nanomaterials by Using Sol-Gel Method

S. S. Butle, G. T. Lamdhade, K. B. Raulkar

Department of Physics, Vidya Bharati Mahavidyalaya, Camp, Amravati

ABSTRACT: In this work, SnO_2, WO_3, and SnO_2-WO_3 hybrid nanomaterials were synthesized via the sol-gel method and characterized for their potential gas-sensing applications. X-ray diffraction (XRD) analysis confirmed the successful formation of crystalline SnO_2 (rutile phase) and WO_3 (monoclinic phase), with the hybrid composites, NC-1 (20% SnO_2 - 80% WO_3), NC-2 (40% SnO_2 - 60% WO_3), and NC-3 (60% SnO_2 - 40% WO_3), displaying diffraction peaks from both materials, indicating a well-integrated structure. Scanning electron microscopy (SEM) revealed uniform spherical nanoparticle morphologies with an average size range of 15–30 nm, which are favorable for enhancing gas-sensing performance. The gas-sensing behavior of the nanomaterials was evaluated for various gases, demonstrating superior sensitivity and faster response times for the SnO_2-WO_3 hybrid composites compared to the individual oxides. Among the hybrids, NC-2 (40% SnO_2 - 60% WO_3) exhibited the best gas-sensing performance, highlighting the synergistic effect of combining SnO_2 and WO_3 in enhancing gas-sensing properties [1-3]. These results make the SnO_2-WO_3 hybrid materials promising candidates for future gas detection applications.

KEYWORDS: Gas sensors; nanomaterials; tungsten oxide; tin oxide; SnO_2-WO_3; air quality monitoring.

I. INTRODUCTION

Metal-oxide nanomaterials-especially SnO_2 (tin oxide) and WO_3 (tungsten oxide) have attracted significant interest due to their distinctive chemical and physical properties. Their high efficiency, stability, affordability, and non-toxic nature make them valuable in applications such as catalysis, optical devices, chemical and biosensors, and various nanodevices. SnO_2, WO_3, and their hybrid nanocomposites (SnO_2–WO_3) demonstrate particularly strong gas-sensing capabilities. This enhanced performance results from their open, sponge-like porous morphology, which increases surface reactivity and promotes efficient gas interaction. Numerous synthesis approaches—including solid-state, electrochemical, hydrothermal, sonochemical, green methods, and thermal evaporation have been used to produce these nanomaterials [4-6].

In this study, we introduce a simple and cost-effective method for preparing SnO_2 and SnO_2–WO_3 nanocomposites with varying stoichiometric ratios: NC-1 (20% SnO_2, 80% WO_3), NC-2 (40% SnO_2, 60% WO_3), and NC-3 (60% SnO_2, 40% WO_3). Their structural and morphological characteristics were analyzed, and their gas-sensing performance was evaluated. Among the composites, NC-2 exhibited the highest sensitivity and fastest response. These findings demonstrate the strong potential of SnO_2–WO_3 hybrid nanomaterials for advanced gas detection and environmental monitoring applications [7-10].

II. RESEARCH REVIEW

SnO_2 and WO_3 are widely studied metal-oxide semiconductors known for their strong gas-sensing properties, thermal stability, and high surface reactivity. Earlier research shows that combining these oxides into SnO_2–WO_3 hybrid nanomaterials enhances sensitivity and response speed due to improved charge transfer, increased active sites, and synergistic interactions between the two phases. Various synthesis methods have been reported, but the sol–gel technique remains preferred for its simplicity, cost-effectiveness, and ability to produce uniform nanoparticles. Previous studies also confirm that the crystalline structures of SnO_2 (tetragonal) and WO_3 (monoclinic) contribute significantly to their sensing performance. However, further investigation is needed to optimize composition ratios and understand their influence on gas-sensing behavior. This research addresses these aspects by preparing and characterizing SnO_2, WO_3, and SnO_2–WO_3 composites using the sol–gel method.

International Journal of Advanced Research in Science, Engineering and Technology
ISSN: 2350-0328
Vol. 12, Special Issue, December 2025
National Conference on Earth, Elements and Energy: Interdisciplinary Perspectives (NC3EIP–2025)
IJARSET IMPACT FACTOR 7.150

III. MATERIALS AND METHODS

A. Preparation of SnO_2, WO_3 and SnO_2-WO_3 nanocomposites

SnO_2 nanoparticles were prepared via a sol-gel process by dissolving $SnCl_4 \cdot 5H_2O$ in double-distilled water and ethylene glycol at 60°C. NH_4OH was added dropwise to form a white gel, which was ultrasonicated, filtered, washed, and dried at 120 °C for 24 hours to yield SnO_2 nanoparticles [11-12].

WO_3 nanoparticles were synthesized via a sol-gel method. WCl_6 was dissolved in ethanol to form $W(OC_2H_5)_6$, followed by addition of NH_4OH and 24 hours of stirring under ice-cooling to induce hydrolysis. The resulting precipitate was washed, centrifuged until chloride-free (verified with $AgNO_3$), and then peptized with additional ammonium hydroxide. To improve colloidal stability, 50 µL of Triton X-100 was added, allowing the WO_3 gel to form. The gel was spin-coated onto a cleaned alumina substrate at 500 rpm for 30 s and then 2000 rpm for 90 s, producing a uniform coating. The WO_3-coated alumina substrates were calcined at 300–600 °C for 1 hour, then slowly cooled in the furnace to obtain well-crystallized WO_3 arrays with improved structural ordering [13-14].

SnO_2–WO_3 nanocomposites were synthesized by mixing stoichiometric amounts of Sn and W precursors in a solvent system of water and ethylene glycol. The mixture underwent the sol-gel process, where ammonia was added to induce hydrolysis and condensation. The resulting gel was dried and calcined to form the SnO_2–WO_3 composite nanoparticles. The uniform mixing of SnO_2 and WO_3 at the molecular level resulted in well-dispersed composite powders with enhanced properties [15-16].

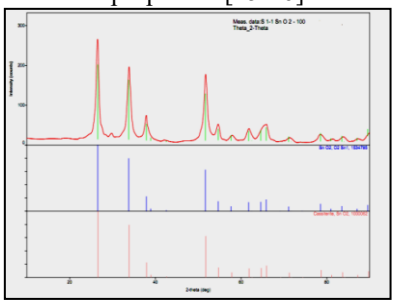
Fig. 1 XRD 100%SnO_2

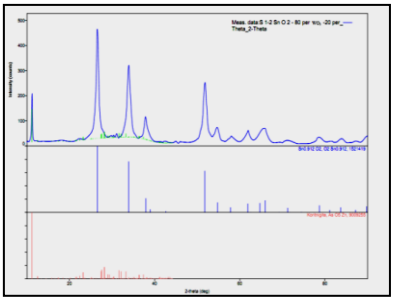
Fig. 2 XRD 20%SnO_2- 80% WO_3

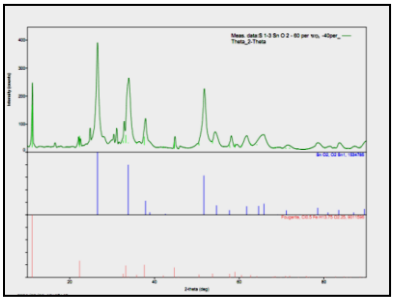
Fig. 3 XRD 40%SnO_2- 60% WO_3

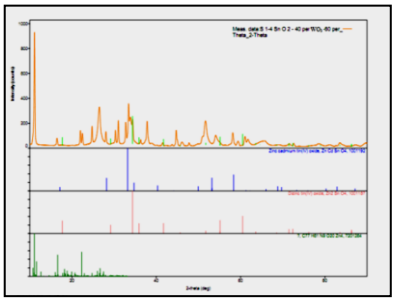
Fig. 4 XRD 60%SnO_2- 40% WO_3

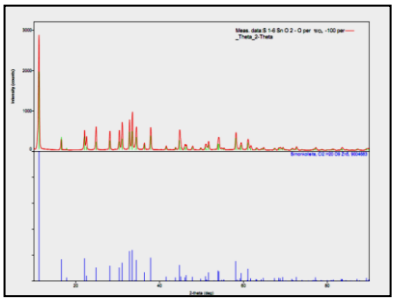
Fig. 5 XRD 100% WO_3

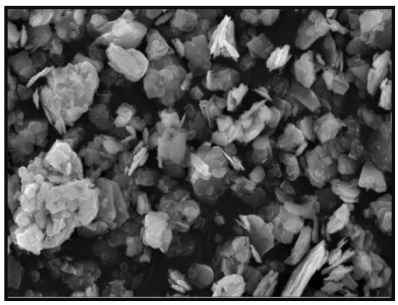
Image 1 SEM 100%SnO_2

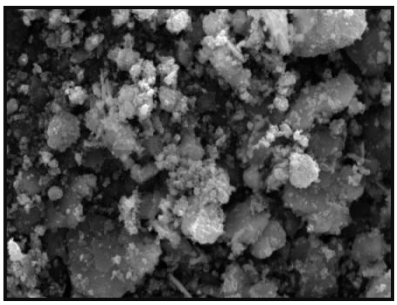
Image 2 SEM 20%SnO_2- 80% WO_3

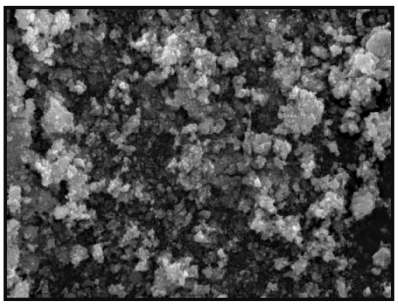
Image 3 SEM 40%SnO_2-60%WO_3

International Journal of Advanced Research in Science, Engineering and Technology
ISSN: 2350-0328
Vol. 12, Special Issue, December 2025
National Conference on Earth, Elements and Energy: Interdisciplinary Perspectives (NC3EIP–2025)
IJARSET IMPACT FACTOR 7.150

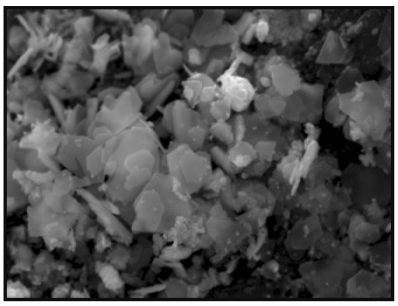
Image 4 SEM 60%SnO_2-40% WO_3

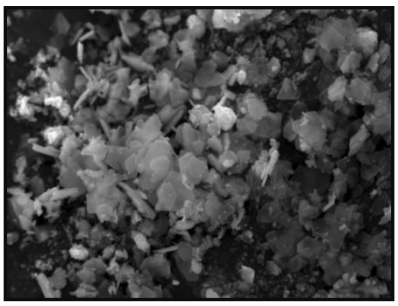
Image 5 SEM 100%WO_3

B. Characterization

SnO_2, WO_3, and SnO_2–WO_3 hybrid nanomaterials were synthesized via the sol–gel method and characterized using XRD and SEM. XRD analysis confirmed their crystalline nature, with SnO_2 showing tetragonal rutile peaks and WO_3 exhibiting a monoclinic phase. The hybrid composite displayed peaks from both oxides, indicating successful composite formation without impurities. Crystallite sizes calculated by the Scherrer equation were within the nanometer range. SEM images revealed uniformly distributed, nearly spherical nanoparticles with slight agglomeration. The SnO_2–WO_3 composite showed a more interconnected and compact morphology, demonstrating effective mixing and interaction between the two oxide phases [15-16].

IV. CONCLUSION

In conclusion, SnO_2, WO_3, and SnO_2–WO_3 hybrid nanomaterials were successfully synthesized using the sol–gel method, a simple, cost-effective technique for producing highly crystalline nanostructures. XRD analysis confirmed the formation of pure SnO_2 (tetragonal rutile) and WO_3 (monoclinic) phases, while the hybrid composites showed peaks from both oxides, indicating successful integration without impurities. SEM images revealed uniform, spherical nanoparticles with well-connected surface morphology, particularly in the hybrid samples. The NC-2 (40% SnO_2–60% WO_3) composite exhibited enhanced gas-sensing properties, including higher sensitivity and faster response times, highlight the potential of these hybrid materials for gas detection and environmental monitoring [17-18].

REFERENCES

1. Ksenija Maver , Iztok Acon, Mattia Fanetti, Samar Al Jitan , Giovanni Palmisano, Matjaz Valant, Urska Lavreni Stangar, Improved photocatalytic activity of SnO_2-TiO_2 nanocomposite thin films prepared by low-temperature sol-gel method, Catalysis Today 397-399 **(2022)** 540–549, https://doi.org/10.1016/j.cattod.2021.06.018.
2. Y. Yang, H. Li, H. Zhao, R. Qu, S. Zhang, W. Hu, X. Yu, X. Zhu, S. Liu, C. Zheng, X. Gao, Structure and crystal phase transition effect of SnO_2 doping on anatase TiO_2 for dichloromethane decomposition, J. Hazard. Mater. 371 **(2019)** 156–164, https://doi.org/10.1016/j.jhazmat.2019.02.103
3. K. Awa, R. Akashi, A. Akita, S. ichi Naya, H. Kobayashi, H. Tada, Highly efficient and selective oxidation of ethanol to acetaldehyde by a hybrid photocatalyst consisting of SnO_2 nanorod and rutile TiO_2 with heteroepitaxial junction, Chem. Phys. Chem. 20 **(2019)** 2155–2161, https://doi.org/10.1002/cphc.201900632
4. W. Sangchay, The self-cleaning and photocatalytic properties of TiO_2 doped with SnO_2 thin films preparation by sol-gel method, Energy Procedia 89 **(2016)** 170–176, https://doi.org/10.1016/j.egypro.2016.05.023.
5. A. Kusior, L. Zych, K. Zakrzewska, M. Radecka, Photocatalytic activity of TiO_2/ SnO_2 nanostructures with controlled dimensionality/complexity, Appl. Surf. Sci. 471 **(2019)** 973–985, https://doi.org/10.1016/j.apsusc.2018.11.226.
6. I. Rangel-V´ azquez, G. Del Angel, V. Bertin, F. Gonz´ alez, A. Vazquez-Zavala, A. Arrieta, J.M. Padilla, A. Barrera, E. Ramos-Ramirez, Synthesis and characterization of SnO_2 doped TiO_2 photocatalysts: effect of SnO_2 concentration on the textural properties and on the photocatalytic degradation of 2,4-dichlorophenoxyacetic acid, J. Alloy. Compd. 643 (**2015**) S144–S149, https://doi.org/10.1016/j.jallcom.2014.12.065
7. H. Jamalabadi, N. Alizadeh, Enhanced low-temperature response of PPy-WO_3 hybrid nanocomposite based gas sensor deposited by electrospinning method for selective and sensitive acetone detection, IEEE Sensor. J. 17 (8) **(2017)** 2322–2328, https://doi.org/10.1109/jsen.2017.2662716.
8. T.T.N. Hoa, D.T.T. Le, N. Van Toan, N. Van Duy, C.M. Hung, N. Van Hieu, N.D. Hoa, Highly selective H2S gas sensor based onWO_3-coated SnO_2 nanowires,Mater. Today Commun. 26 **(2021)** 102094, https://doi.org/10.1016/j.mtcomm.2021.102094.
9. G. Jung, S. Hong, Y. Jeong, W. Shin, J.-W. Park, D.H. Kim, Highly selective and low-power carbon monoxide gas sensor based on the chain reaction of oxygen and carbon monoxide to WO_3, ACS Appl. Mater. Interfaces **(2022),** https://doi.org/10.1021/acsami.1c25221
10. H. Ji, W. Zeng, Y. Xu, Y. Li, Nanosheet-assembled hierarchical WO_3 flower-like nanostructures: hydrothermal synthesis and NH3-sensing properties, Mater. Lett. 250 **(2019)** 155–158, https://doi.org/10.1039/c8ra01818a.
11. H. Jamalabadi, N. Alizadeh, Enhanced low-temperature response of PPy-WO_3 hybrid nanocomposite based gas sensor deposited by electrospinning method for selective and sensitive acetone detection, IEEE Sensor. J. 17 (8) **(2017)** 2322–2328, https://doi.org/10.1109/jsen.2017.2662716.

International Journal of Advanced Research in Science, Engineering and Technology

ISSN: 2350-0328

Vol. 12, Special Issue, December 2025

National Conference on Earth, Elements and Energy: Interdisciplinary Perspectives (NC3EIP–2025)

IMPACT FACTOR 7.150

12. Govindaraj, T., Mahendran, C., Manikandan, V. S., Archana, J., Shkir, M., & Chandrasekaran, J. **(2021).** Fabrication of WO_3 nanorods/RGO hybrid nanostructures for enhanced visible-light-driven photocatalytic degradation of Ciprofloxacin and Rhodamine B in an ecosystem. Journal of Alloys and Compounds, 868, Article 159091. https://doi.org/10.1016/j.jallcom.2021.159091
13. Huang, S., Bao, R., Wang, J., Yi, J., Zhang, Z., Liu, L., Han, Y., Li, Z., Min, D., Zhang, W., Ge, Z., & Zhang, X. **(2023).** Synergistic effect of oxygen vacancy defects and TiO2/ WO_3 heterostructures in photocatalytic hydrogen production and dye degradation. Journal of Alloys and Compounds, 961, Article 170945. https://doi.org/10.1016/j.jallcom.2023.170945.
14. A. Sharma, S. Arya, B. Singh, P. Tomar, S. Singh, R. Sharma, Sol-gel synthesis of Zn- doped MgO nanoparticles and their applications, Integrated Ferroelectrics Int. J. 205 (1) **(2020)** 14–25, https://doi.org/10.1080/10584587.2019.1674993.
15. K. Ahmed, M. Kumar, others, Optical and structural properties of Mn-doped MgO powders synthesized by sol-gel process, Optik 127 (20) **(2016)** 8253–8258, https://doi.org/10.1016/j.ijleo.2016.06.055.
16. N. Bayal, P. Jeevanandam, Synthesis of TiO_2–MgO mixed metal oxide nanoparticles via a sol-gel method and studies on their optical properties, Ceram. Int. 40 (10) **(2014)** 15463–15477, https://doi.org/10.1016/j.ceramint.2014.06.122.
17. S. Abinaya, H.P. Kavitha, Magnesium oxide nanoparticles: effective antilarvicidal and antibacterial agents, ACS Omega 8 (6) **(2023)** 5225–5234, https://doi.org/10.1021/acsomega.2c01450.
18. R.S. Ingale, S.G. Shinde, K.A. Khamkar, S.A. Ahire, I.J. Patil, The Al^{3+} doped modified ZnO sensor material: fabrication, characterization, and gas sensing characteristics of some environmental pollutant and greenhouse gases, J. Phys. Conf. 2426 (1) (**2023,** February) 012050, https://doi.org/10.1088/1742-6596/2426/1/012050.